International Journal of Pharmaceutics 641 (2023) 123048

Contents lists available at ScienceDirect

International Journal of Pharmaceutics

journal homepage: www.elsevier.com/locate/ijpharm

Contact lenses that transform gold into nanoparticles for prophylaxis of light-related events and photothermal therapy

Carmen Alvarez-Lorenzo *, Maria Vivero-Lopez, Angel Concheiro

Departamento de Farmacología, Farmacia y Tecnología Farmacéutica, I+DFarma Group (GI-1645), Facultad de Farmacia, Instituto de Materiales (iMATUS), and Health Research Institute of Santiago de Compostela (IDIS), Universidade de Santiago de Compostela, 15872 Santiago de Compostela, Spain

ARTICLE INFO

Keywords:
Contact lenses
Gold nanoparticles
Silicone hydrogel
Photothermal therapy
Autoclave
Light-filter medical device
Anisotropic gold particles

ABSTRACT

This work describes for first time how anisotropic gold nanoparticles (AuNPs) can be spontaneously formed inside preformed contact lenses (CLs) avoiding the use of additional reductant agents (reagent-free) through a precise tunning of the monomeric composition, the saline concentration, and the application of steam heat sterilization. Protocols to generate AuNPs in solution using inorganic or small organic reductants are widely available. Differently, gold precursors interactions with polymer networks have been overlooked and, thus, the interest of chemically cross-linked hydrogels as organic reductants is still to be elucidated. In the ocular field, incorporation of AuNPs to CLs may expand their applications in prophylaxis, therapy and diagnosis. To carry out the work, a variety of hydrogels and commercially available CLs were incubated with gold salt solution without any other chemical reagent. AuNPs formation was monitored by changes in localized surface plasmon resonance (LSPR) bands and quantifying the gold sorbed. Only silicone hydrogels induced AuNPs formation at room temperature in few days; methacrylic acid red-shifted the LSPR band (550–600 nm), while monomers bearing F hindered the reduction. Storage of hydrogels in the gold precursor solution allowed a gradual formation of anisotropic AuNPs, which could be stopped at any time by washing the hydrogel with water. The developed CLs behave as efficient filters against highly penetrant light and also exhibit photoresponsiveness as demonstrated as rapid (10 s), focused mild hyperthermia when irradiated with green, red and NIR lasers.

1. Introduction

Gold nanoparticles (AuNPs) are being tested as components of a wide range of medical devices to expand their use in prophylaxis, therapy and diagnosis. AuNPs can endow medical devices with antibacterial and antibiofilm features, serve as imaging agents for accurate localization and as electrochemical biosensors for in vivo real-time monitoring of biomarkers, and are suitable for localized photothermal therapy, among other functionalities specially if the AuNPs are anisotropic (Cabana et al., 2017; Cho et al., 2021; Li et al., 2014; Peris-Martinez et al., 2021, Piktel et al., 2021; Zhang et al., 2019). Although still little explored, contact lenses (CLs) and intraocular lenses (IOLs) may be particularly suitable devices for the full development of AuNPs performances due to their accessibility to different light sources and transparency (Peris-Martinez et al., 2021).

In the ocular field, CLs containing AuNPs may find novel applications as light filters, sensors for eye diseases, and photothermal therapy. The extended use of digital screens and lasers in a wide variety of fields, covering from domestic to industrial environments, pose a threat for human ocular health (Public Health England, 2016; Bhavsar et al., 2021). CLs that can partially block sun light radiation of short wavelengths are commercially available, and new UV filters are under development process (Kapfelsberger et al., 2021). Differently, less protection is available against the most penetrant red and near infrared radiation (NIR), which can easily get access to the posterior segment of the eye and damage the retina. To partially address this problem, incorporation of gold nanoparticles (AuNPs) to ocular bandages, especially CLs, has recently been proposed as a way to protect from green lasers (Liu and Chauhan, 2022; Mariño-López et al., 2019). CLs with light filters in specific wavelength regions may find the additional function of helping people that are blind to certain colors (Salih et al., 2021). To be useful as red light and NIR blockers inside CLs, the AuNPs should absorb the unwanted radiation without causing excessive increase in temperature. Nevertheless, small increments in temperature, i.e., few degrees above eye surface temperature (up to 41–44 °C), are not a problem and may even have beneficial effects to manage dry eye

* Corresponding author.
E-mail address: carmen.alvarez.lorenzo@usc.es (C. Alvarez-Lorenzo).

https://doi.org/10.1016/j.ijpharm.2023.123048
Received 21 March 2023; Received in revised form 9 May 2023; Accepted 9 May 2023
Available online 14 May 2023

symptoms since heat favors fluidification of lipids on the internal face of the lids (Beining et al., 2022). Photothermal therapy can also be exploited against eye tumors on the anterior segment (Luo et al., 2015) and for prevention and management of posterior capsule opacification associated to IOLs (Lin et al., 2017). In any case, for the feasibility of use, the CL must still allow for penetration of light in the mid-region of visible spectrum to enable accurate vision. The labile equilibrium between the sorption of a desired radiation wavelength and the sufficient transmittance of light required for vision may strongly depend on the homogeneous distribution of low proportions of AuNPs of right shape and size in the bulk of the CL (Link and El-Sayed, 2000).

Three different approaches have been tested so far to load AuNPs into CLs: (a) AuNPs are prepared in advance and then added to the CL monomers before polymerization (Li et al., 2021a; Mariño-López et al., 2019; Mariño-López et al., 2022; Salih et al., 2021); (b) AuNPs and CLs are prepared in separate and then the CLs are soaked into AuNPs dispersions (Li et al., 2021a); or (c) preformed CLs are soaked into gold precursors and then a strong reductant inorganic chemical agent is added to trigger AuNPs formation in the hydrogel bulk (Liu et al., 2021). These approaches have been demonstrated to be useful for diverse applications, including performance as sensors, enhanced loading of drugs, capture of cystine, and blocking of green light (Li et al., 2021a; Liu and Chauhan, 2022; Liu et al., 2021). Each approach has its own advantages and limitations, although most protocols are coincident in the fact that they render small spherical AuNPs that absorb in the 520–550 nm region which constrains light-related applications (Li et al., 2014).

Preparation of AuNPs in separate (options a and b) has the advantage of the versatility of techniques that can be applied to produce AuNPs of desired size and shape but has the drawback of the many steps required to obtain the final product (CL + AuNPs). Addition of AuNPs during CL fabrication alters common manufacture protocols and may also modify the polymerization process, which means the implementation of additional quality control protocols during CL production. Loading of AuNPs into preformed CLs by soaking demands time for the AuNPs to diffuse into the CL bulk and does not ensure retention of the AuNPs inside the CL unless chemical interactions between both materials occur. It should be noted that, although AuNPs have demonstrated an adequate safety profile as ocular drug carriers, the continuous leakage of AuNPs during CL wearing may cause off-target accumulation in eye tissues with unpredictable long-term response (Masse et al., 2019; Sonntag et al., 2021). Option (c) has the advantage of being applicable to any CL since the AuNPs are forced to be formed inside the CL using strong inorganic reductants, but as drawbacks these reagents may damage the polymer network of the CL and require intense washing protocols to avoid traces of the reducing agent that compromise ocular safety. Moreover, the control on size and shape of the internally formed AuNPs is minor since small spherical nanoparticles are mostly generated, which limits the tuning of the wavelength that the AuNPs can absorb.

Compared to inorganic reductant agents, organic reductants are receiving increasing interest as more eco-friendly and cheaper alternatives (Okonkwo et al., 2021; Zhang et al., 2013). Aqueous dispersions of poly(ethylene oxide)-poly(propylene oxide)-poly(ethylene oxide) copolymers (Goy-Lopez et al., 2010; Sakai and Alexandridis, 2005) and polyvinyl alcohol (Alvarez-Lorenzo et al., 2020) induce the nucleation of AuNPs and regulate their controlled growth toward a variety of anisotropic nanostructures. The reaction does not require catalyzers or other reagents, and thus stable hybrid polymer-AuNPs can be obtained in one step in the absence of downstream purification processes. Radiations and moderate heating have been shown to be useful to accelerate the reduction (Porel et al., 2005). So far these hybrid colloidal systems have been tested as gel depots for localized photothermal ablation and as theranostic nanodevices (Cabana-Montenegro et al., 2019).

In the previous reports on CL + AuNPs the interactions of the CL components with the gold precursors have been overlooked. In parallel, the reduction of metal ions with polymers has been studied in one-phase (namely polymer solution) (Dumur et al., 2011; Zhang et al., 2013) while the advantages or constrains of using chemically cross-linked networks as organic reductants have scarcely been evaluated (Li et al., 2021b). Thus, the aim of this work was to elucidate the effects that the composition of the CL cross-linked network and the conventional sterilization process (steam heat) may have on the spontaneous formation of AuNPs inside preformed CLs. It can be hypothesized that the oxidant/reductant nature of CL components may play a relevant role in the yield of AuNPs formation and their morphological features (mainly, size and anisotropy) which are critical for subsequent applications. Also, the steam heat conditions commonly applied for sterilization of CLs could accelerate the spontaneous formation of AuNPs if the polymer network contains chemical groups that can aid in the reduction and nucleation of gold salts. To carry out the work a wide variety of hydrogels prepared with different monomers typically used as components of CLs were synthesized and incubated with gold salt solution without the addition of any other chemical reagent (reagent-free). Commercially available CLs were also investigated in parallel. Then, the hydrogels and CLs were steam heat sterilized and the changes underwent by gold species both in the solvent medium and inside the polymer network were investigated. An additional aim was to elucidate the role that other salt ions (e.g., NaCl) may have in the gold reduction process. NaCl 0.9 % is commonly used to adjust osmotic pressure of CL packaging solutions, but the salt ions might compete with gold ions for binding to the polymer network and thus interfere in the reduction process. Localized surface plasmon resonance (LSPR) bands were monitored over time before and after autoclaving in salt-free and salt-containing solutions. Finally, the photoresponsive capability of the newly formed CL + Au hybrid material was investigated in terms of focused mild hyperthermia during irradiation with lasers covering a wide range of wavelengths (green, red and NIR at 808 nm).

2. Materials and methods

2.1. Materials

Hydrogen tetrachloroaurate(III) ($HAuCl_4$), ethylene glycol dimethacrylate (EGDMA), dichlorodimethylsilane, benzyl methacrylate (BzMA), ethylene glycol phenyl ether methacrylate (EGPEM), methacrylic acid (MAA), 2-acrylamido-2-methylpropane sulfonic acid (AMPSA) and 2,2′-azobis(2-methylpropionitrile) (AIBN) were from Sigma Aldrich (St Louis, MO, USA). 2-Hydroxyethyl methacrylate (HEMA) was from Merck KGaA (Darmstadt, Germany). N-(3-aminopropyl) methacrylamide hydrochloride (APMA) was from PolySciences Inc. (Warrington, Pennsylvania, USA). Monomethacryloxypropyl-*sym*-polydimethylsiloxane hydroxypropyl terminated (MCS-MC12) was from Gelest, Inc (Morrisville, PA, USA).

Distilled water was used for all experiments. All other reagents were analytical grade. Commercially available CLs were Esencia® 50 (acolfilcon B; base curvature 8.6; diameter 14.0; power −5.0) from Eurolent Servicios Ópticos S.L. (Madrid, Spain), Unisil (silicone hydrogel; base curvature 8.8; diameter 14.5; power + 3.0) from Contamac UK, Biofinity Energys™ (BE; comfilcon A 52 %; base curvature 8.6; diameter 14.0; power −6.0, −2.5 and + 1.5) from Cooper Vision (Hamble, UK), Acuvue® Oasys with HydraLuxe™ (senofilcon A; base curvature 8.5; diameter 14.3; power −3.00) from Johnson & Johnson Vision Care Company (Limerick, Ireland), and 1-Day Acuvue® Moist® with Lacreon® (etafilcon A; base curvature 8.5; diameter 14.2; power −3.00) from Johnson & Johnson Vision Care Company (Limerick, Ireland). Commercial CLs were acquired from local optician's shops and were extensively washed with water in individual baskets for 24 h and dried at 50 °C for 12 h before testing.

2.2. Hydrogel synthesis

Various hydrogel batches differing in the structural monomers (Fig. 1) were prepared with the compositions shown in Table 1, as

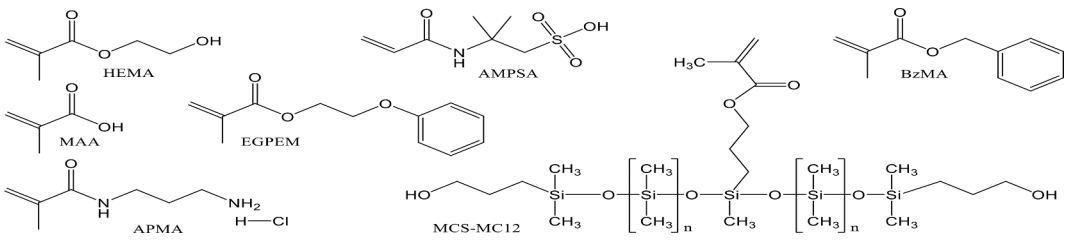

Fig. 1. Monomers used as components of the hydrogel and silicone hydrogel contact lenses.

Table 1
Monomers mixtures used to prepare the hydrogels. DMSO (0.5 mL) and AIBN (8.2 mg) were added to each H, B and S mixture to facilitate AMPSA solubilization and to serve as initiator, respectively. For AE series, DMSO was not used, and AIBN was 4.93 mg.

Hydrogel code	HEMA (mL)	BzMA (μL)	MCS-MC12 (μL)	MAA (μL)	AMPSA (mg)	EGPEM (μL)	APMA (mg)	EGDMA (μL)
H1	4	–	–	–	–	–	–	6.04
H2	4	–	–	34.4	–	–	–	6.04
H3	4	–	–	68.9	–	–	–	6.04
H4	4	–	–	–	83.0	–	–	6.04
H5	4	–	–	–	166.0	–	–	6.04
B1	4	141	–	–	–	–	–	6.04
B2	4	141	–	34.4	–	–	–	6.04
B3	4	141	–	68.9	–	–	–	6.04
B4	4	141	–	–	83.0	–	–	6.04
B5	4	141	–	–	166.0	–	–	6.04
S1	3.5	–	500	–	–	–	–	12.08
S2	3.5	–	500	34.4	–	–	–	12.08
S3	3.5	–	500	68.9	–	–	–	12.08
S4	3.5	–	500	–	83.0	–	–	12.08
S5	3.5	–	500	–	166.0	–	–	12.08
AE1	3	–	–	–	–	112.50	–	12.08
AE2	3	–	–	–	–	112.50	21.45	12.08
AE3	3	–	–	–	–	–	21.45	12.08

previously described (Pereira-da-Mota et al., 2021). Briefly, the monomers solutions were injected in glass molds (12x14 cm) prepared with a teflon frame of 0.2 mm thickness, and the polymerization was carried out at 50 °C for 12 h and at 70 °C for other 24 h. Then, the hydrogels were boiled, cut as 10 mm discs, and extensively washed until no monomer leakage was detected. The discs were dried at 70 °C for 24 h. Hydrogels coded as H, B, and AE corresponded to common compositions of hydrogel soft CLs, while hydrogels coded with S correspond to silicone hydrogel CLs. A second batch of S silicone hydrogels was synthesized without AMPSA and in the absence of DMSO; this second batch was designed as S1b, S2b and S3b as had the same compositions as those of S1, S2 and S3, but without using DMSO.

2.3. Preparation of CL + Au hybrid system

Before the experiments all glassware was carefully washed with HCl 10 mM and then rinsed with distilled water to remove potentially interfering ions. Dried hydrogel discs or CLs were weighed and individually placed in freshly prepared $HAuCl_4$ solution in water. Two different concentrations and volumes were tested (a) 0.655 mM, 1 mL; and (b) 0.327 mM, 2 mL. Six replicates of each disc or CL were evaluated in each condition. The vials were capped and stored for 72 h at room temperature protected from light. Special attention was paid to that the entire disc or CL remained totally immersed in the $HAuCl_4$ solution. Light transmission of the discs and CLs after storage was evaluated in the 200–900 nm range (1 nm step) using an Agilent Cary 60 UV–Vis spectrophotometer (Santa Clara, CA, USA). The discs and CLs were immediately returned to the $HAuCl_4$ solution, and the vials were sealed and autoclaved at 121 °C for 15 min. Then, the vials were left to equilibrate at room temperature for 4 h, and the light transmission of the discs and CLs was recorded again. Finally, discs and CLs were rinsed with water and transferred to Eppendorf tubes containing distilled water or NaCl 0.9 % medium (4 mL).

The pH values of the $HAuCl_4$ aq. solution were recorded before and after steam heat sterilization both in the presence and in the absence of the discs and CLs. Water uptake by the discs and CLs was quantified after 3 days incubation in the $HAuCl_4$ solution (0.327 mM, 2 mL) and subsequent sterilization, as follows.

$$\text{Water content}(\%) = \frac{Ww - Wd}{Ww} \quad (1)$$

In this Equation, *Wd* represents the weight of the dried disc or CL before the treatment and *Ww* is the weight of the disc or CL after incubation in the $HAuCl_4$ solution and subsequent sterilization.

2.4. Gold remaining in the solution

The UV–Vis spectra of gold solutions were recorded in the 190–800 nm range (Agilent 8453, Germany) before and after being autoclaved in the presence and absence of the hydrogels.

2.5. Gold inside the hydrogels

Hydrogels were washed with water and freeze-dried before X-ray and Field Emission Scanning Electron Microscopy with Energy Dispersive X-Ray Spectroscopy (FESEM-EDX) analysis. Crystalline powder X-ray diffraction (XRPD) data were obtained using a Bruker D8 Advance diffractometer (40 kV, 40 mA, theta/theta) equipped with an X-ray tube of sealed Cu (CuKα1; λ = 1.5406 Å) and a LYNXEYE EQUIST-type detector. The diffractograms were obtained in the angular range of 3 to 70º with a step of 0.02º and a time per step of 2 s, and the diffractograms obtained were analyzed using HighScore Plus, version 3.0d software. Scanning electron microscopy (SEM) images and microanalysis were recorded in a ZEISS GEMINI-500 (BSD4 detector) with EDX (UltimMax-170; Oxford, 127ev) at various magnifications. Original SEM images were transformed to JPG file and the circularity of the particles was

calculated using ImageJ 1.53 k free software (Schneider et al., 2012). Transmittance spectra of S1b, S2b and S3b discs before and after treatment were also recorded in the 200–2000 nm interval (1 nm; 1000 nm/min), after baseline correction in a V-770 UV–Visible/NIR spectrophotometer fitted with VTA-752 sample accessory (Jasco, Tokyo, Japan).

2.6. Effect of contact lens preservation liquid

Aliquots (200 μL or 1 mL) of preservation liquid in which the commercial CLs were supplied were mixed with 0.327 mM $HAuCl_4$ solution in water (2 mL) in glass vials, sealed and stored protected from light at room temperature. The UV–Vis spectra were recorded after three days storage (Agilent 8453, Germany). Then, the solutions were autoclaved at 121 °C for 15 min, the UV–Vis spectra recorded again and the formed AuNPs observed under transmission electron microscopy (TEM).

2.7. Kinetics of AuNPs formation at room temperature

Dried S1b, S2b and S3b silicone hydrogel discs were accurately weighed and placed in 0.327 mM $HAuCl_4$ solution in water (2 mL). The vials were sealed and stored protected from light at room temperature. Absorbance of the gold solution and the discs was monitored, as explained above, along time for five months.

2.8. Reaction in NaCl 0.9 % medium

Dried S1b, S2b and S3b silicone hydrogel discs and commercial CLs directly removed from the original blister (no previous washing or drying) were weighed and immersed in separate in 0.327 mM $HAuCl_4$ solution prepared in NaCl 0.9 % (2 mL). The vials were sealed and stored protected from light at room temperature. After 3 days storage, absorbance of the gold solution and the discs was monitored as reported above. The tests were carried out with 6 replicates. Three replicates were then autoclaved and three were stored at room temperature. The absorbance of the gold solution and the discs was recorded again at different time points during storage.

After 7 days storage, the non-autoclaved silicone hydrogel discs and commercial CLs were removed from the $HAuCl_4$ solution prepared in NaCl 0.9 %, washed for 3 days in water, and transferred to $HAuCl_4$ solution in water (0.327 mM, 2 mL). The vials were sealed and stored protected from light at room temperature. Absorbance of the gold solution and the discs was monitored along time for five months.

2.9. Laser light transmission and photothermal responsiveness

Responsiveness of the discs with and without AuNPs to light was evaluated using three laser pointers covering a wide range of wavelengths: a bullet 100 mW green laser pointer 532 nm (beam diameter 2.0 mm), a bullet 100 mW red laser pointer 652 nm (beam diameter 2.0 mm), and a IR1 laser pointer 808 nm 100 mW (beam diameter 3.0 mm) (Biglasers.com, Monroe, Ny, USA). Individual discs were placed on a lux light meter sensor (model SBS-LM-400C; Steinberg Systems, Zielona Gora, Poland) and the transmitted radiation was monitored during irradiation. The changes in temperature were also recorded with a FLIR model E75 thermographic camera (Teledyne FLIR LLC, Oregon), taking thermal images at a focal distance of 19 cm at the beginning of the process and after 10 s laser exposure.

3. Results and discussion

3.1. AuNPs formation from precursor in water

A wide variety of cross-linked hydrogels and silicone hydrogels suitable as CLs were synthesized using functional monomers bearing quite different chemical groups (Fig. 1) in order to investigate the effect of the hydrogel composition on the feasibility of *in situ* formation of AuNPs. Also, some commercially available CLs were included in the study. Differently to inorganic reducing agents, organic reductants should first show some chelating or binding ability for the metallic ion. The next step depends on the reductive ability of the organic reducing agent, which can be inferred from the energy of the highest occupied molecular orbital (HOMO) (Sobianowska-Turek et al., 2014). Agents with low standard redox potential (pE^0) can be more likely oxidized, as it is the case of some saccharides and natural acids. Nevertheless, there is a paucity of information on whether the cross-linking can cause changes in the reductive ability of organic reductants due to steric restrictions to the movement and competitive binding in the presence of neighbor chemical groups.

Hydrogel compositions reported in Table 1 had transmittances in the 500–800 nm wavelength region above 90 % (as expected for their use as CLs), which allowed for easy monitoring of AuNPs formation through visual changes in color and UV–vis spectrophotometric recording of transmittance. As a first step, hydrogel discs and CLs were immersed in $HAuCl_4$ (0.327 mM, 2 mL) for 72 h, and changes in the color of the hydrogels and their transmittance as well as the amount of gold ions sorbed by the networks were recorded (Fig. 2). The amounts of gold sorbed by the hydrogels at room temperature are shown as yellow bars in Fig. 2**E**. $HAuCl_4$ (0.327 mM) solution in water (pH 3) showed a yellowish color with a peak in absorbance at 287 nm well in the range of the UV–Vis spectrophotometer measurements (**Figure S1 in Supporting Information**). After 72 h immersion, the absorbance of the medium decreased significantly for all hydrogels except those bearing AMPSA (H4, H5, S4, S5, B4 and B5). Relevantly, AE2 and AE3 discs sorbed almost all gold salt in solution, acquiring yellowish color. S1, S2 and S3 silicone hydrogels (without functional monomers or bearing MAA), which showed intermediate capability to sorb gold, were the only ones that triggered by themselves the formation of AuNPs inside the discs in few hours at room temperature protected from light. These S1, S2 and S3 discs became tinted with the typical red–purple color of AuNPs (**Figure 2 B2**).

Special attention was paid to that the entire disc or CL remained totally immersed in the $HAuCl_4$ solution before steam heat sterilization. Preliminary tests carried out placing the discs in only 1 mL of $HAuCl_4$ (0.655 mM) caused some discs to remain partially attached to the wall of the vials, with only half surface immersed in the gold solution (**Figure S2 in Supporting Information**). The yield of AuNPs formation was clearly different in the portion immersed (which become more tinted) compared to the portion that remained outside the solution during steam heat sterilization (which remained uncolored or faint colored). This finding evidenced that further binding of gold ions to the polymer network occurred during the autoclaving and, therefore, immersion of the hydrogel in the gold solution allowed for further supply of gold inside the hydrogel and enhanced production of AuNPs. To avoid non-homogeneity problems subsequent experiments were carried out with 2 mL gold ions solution (0.327 mM) and the hydrogels remained completely immersed in the solution.

Steam heat sterilization of control $HAuCl_4$ (0.327 mM) aqueous solution caused a minor decrease in the absorbance at 287 nm and non-additional peaks appeared, which indicated that the autoclaving itself did not induce gold reduction neither AuNPs formation in the gold precursor solution in the absence of a reductant agent. The small decrease in absorbance due to autoclaving was taken into account when the amount of gold entrapped by the hydrogels was calculated. In the presence of discs the absorbance of the medium at 287 nm diminished more than 50 %, revealing the high capability of the hydrogels to uptake gold ions (Fig. 2**E, blue bars**). Only hydrogels bearing AMPSA caused the medium to become reddish, showing an increase in the absorbance at 558 nm. This finding suggested the formation of some AuNPs in the solution, which may be due to extraction of polymer components by the acid $HAuCl_4$ solution, which had pH close to 3. Interestingly, the AE2 and AE3 hydrogels that had sorbed almost all gold in solution at room temperature expelled some amount of gold after autoclaving.

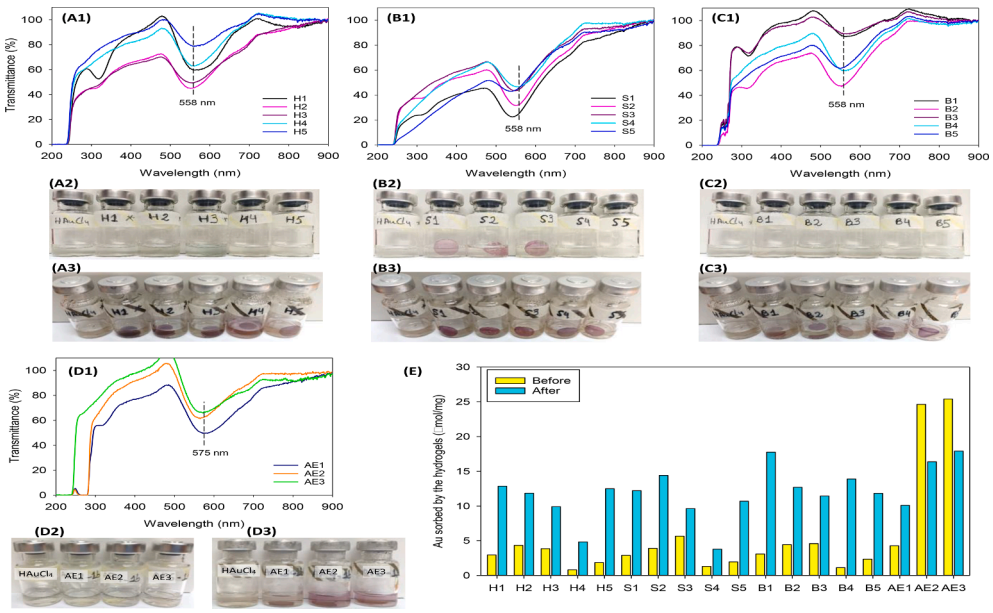

Fig. 2. (A1, B1, C1, D1) Transmittance of the discs after soaking in $HAuCl_4$ solution (0.327 mM, 2 mL) for 72 h and subsequent steam heat sterilization (autoclave, 121 °C, 20 min), and appearance of the same discs before (A2, B2, C2, D2, E2) and after been autoclaved (A3, B3, C3, D3, E3). Only AE2 and AE3 discs became yellow while S1, S2 and S3 discs evidenced a change in color towards light purple before autoclaving. Control $HAuCl_4$ solution maintained the typical slightly yellow color without relevant changes after autoclaving. (E) Amount of gold sorbed by the hydrogels (expressed as μmol per dried mass of the hydrogel) before and after autoclaving estimated from the absorbance of the external aqueous solution. Mean values (n = 3); standard deviations were below 5 %. (For interpretation of the references to color in this figure legend, the reader is referred to the web version of this article.)

Regarding the discs, all compositions depicted in Table 1 underwent a remarkable change in color after steam heat sterilization (Fig. 2 **A3, B3, C3 and D3**). The recording of the light transmission of the discs after sterilization evidenced a decrease in transmittance in the 500–600 nm region, although relevant differences were detected among the tested discs (Fig. 2 **A1, B1, C1 and D1**). Regarding hydrogels without silicone monomer, the presence of low contents in MAA favored the decrease in transmittance in the 558 nm region (hydrogels H2 and B2). In the case of B hydrogels, those prepared with AMPSA had intermediate behavior between non-functionalized and MAA functionalized ones (**Figure 2 C1**). In the case of H hydrogels, those prepared with AMPSA showed the smallest decrease in transmittance in good agreement with the low amount of gold ions trapped (**Figure 2 A1**). Silicone hydrogels S1 (without MAA or AMPSA) underwent the strongest decrease in transmittance, followed by S2 and S3 prepared with MAA. The pronounced drop in transmittance at 558 nm (from 90 % to 20 %) shown by S1 hydrogels incubated for 3 days in $HAuCl_4$ and then steam heat sterilized pointed out these hydrogels as the most efficient ones in terms of gold reductant capability.

Commercially available CLs were previously washed in water for 24 h to remove components from the maintenance liquid that may interfere in the reduction process. CLs made of HEMA hydrogel and minor

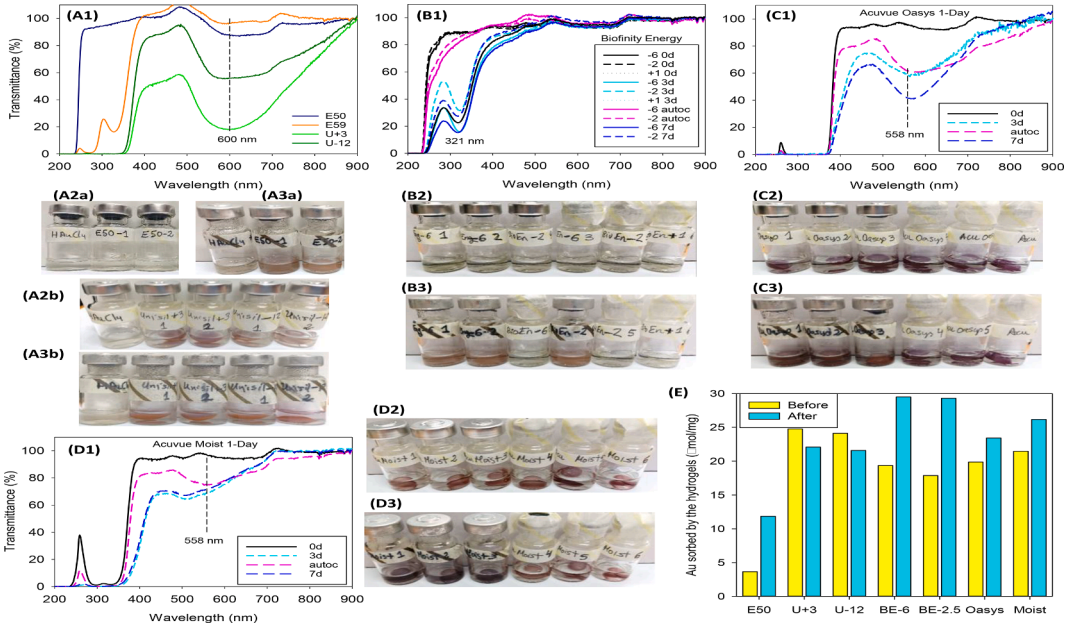

Fig. 3. (A1, B1, C1, D1) Transmittance of the commercial CLs before and after soaking in $HAuCl_4$ solution (0.327 mM, 2 mL) for 72 h. Some replicates underwent steam heat sterilization (autoclave, 121 °C, 20 min; indicated by black strips in the label) and the other replicates were stored until day 7 at room temperature and the transmittance recorded again. Appearance of the same discs before (A2, B2, C2, D2, E2) and after been autoclaved (A3, B3, C3, D3, E3). Unisil CLs (U + 3 and U-12), Acuvue® Oasys and Acuvue® Moist® evidenced a change in color towards light purple before autoclaving. Control $HAuCl_4$ solution maintained the typical slightly yellow color without relevant changes after autoclaving. (E) Amount of gold sorbed by the CLs (expressed as μmol per dried mass of the hydrogel) before and after autoclaving estimated from the absorbance of the external aqueous solution. Mean values (n = 3); standard deviations were below 5 %. (For interpretation of the references to color in this figure legend, the reader is referred to the web version of this article.)

contents in NVP and MMA (Esencia® 50) performed similarly to H discs series (Fig. 3 **A1, A2a, A3a**). Silicone hydrogel Unisil CLs, which contain a non-disclosed mixture of HEMA, NVP, TRIS and SIGMA, sorbed a large amount of gold in solution and transformed it into AuNPs becoming tinted before autoclaving, as observed for silicone hydrogels S1, S2 and S3 (Fig. 3 **A2b, A3b**). Interestingly no relevant differences were observed as a function of the power (dioptor) and both Unisil + 3 and Unisil −12 captured and transformed similar amounts of gold (Fig. 3). Remarkably, Unisil CLs that sorbed large amounts of gold at room temperature did not cause any staining of the liquid medium, confirming that the reduction did progress only inside the CL network. Acuvue® Oasys with HydraLuxe™, which is made of senofilcon A and contains 9.7–12.8 % Si in the outermost region of the CL (Rex et al., 2018), performed similarly to Unisil CLs and triggered an intense formation of AuNPs after 3 days in the gold ions solution (Fig. 3 **C1, C2**). The CLs became more intensely colored after autoclaving.

Surprisingly, Biofinity Energys™ did not induce the reduction of gold despite being a silicone hydrogel too. These CLs are made of comfilcon A, a mixture of siloxanes and silicones with an elemental composition of 10.8–16.5 % Si and 2.5–3.4 % F in the outermost region of the CL (Rex et al., 2018). Thus, it is the only CL with a remarkable content in fluorine. As observed for hydrogels AE2 and AE3 bearing amino moieties, the Biofinity Energys™ CLs showed a remarkably high capability to uptake gold ions but failed to transform them into AuNPs. These CLs required steam heat sterilization for the triggering of AuNP formation, but even after the heating the staining was faint. No differences in reductive ability were detected among dioptors or incubation time in the gold ions solution (Fig. 3 **B1-B3**).

Another unexpected behavior was found for 1-Day Acuvue® Moist® with Lacreon® which is made of etafilcon A, i.e. a copolymer of HEMA and MAA cross-linked with EGDMA and 1,1,1-trimethylol propane trimethacrylate. These CLs contain a permanent water-holding agent, polyvinyl pyrrolidone (PVP), which is claimed to be not released to the medium (Sheardown et al., 2006) and has previously been demonstrated able to induce AuNPs formation by itself (Xan et al., 2010). These CLs reduced gold at room temperature and became reddish after 3 days storage before autoclaving (Fig. 3 **3 D1, D2**). Interestingly, the color shifted towards higher wavelengths after autoclaving, becoming more purple (like Acuvue® Oasys). It should be noted that recording the transmittance of commercial CLs was quite tricky because of changes in thickness along the curvature radius, and thus the percentage of transmittance varied from the center (less tinted) towards the outer end (more tinted).

After sterilization of the discs the pH of the medium was measured again (pH ~ 3), and the discs were transferred to distilled water or NaCl 0.9 % medium. After one week storage, the medium did not show absorbance in the 200–800 nm range which meant that the AuNPs did not leach from the hydrogels. Also, the transmittance pattern of the stored discs with AuNPs formed inside did not change after soaking in distilled water or NaCl 0.9 % medium for one week and remained the same six months later.

The differences in the ability of the hydrogel networks to reduce gold could be explained on the basis of the information available for single components, as follows. A variety of small organic carboxylic acids (succinic, ascorbic,…) have demonstrated excellent reducing ability due to their low pE^0 values, associated to the easily oxidized enediol group (Okonkwo et al., 2021). The reaction rate was shown to depend on the number of hydroxyl groups since they accelerate the reaction. Predominance of carboxylic acid groups (in detriment of hydroxyl ones) makes the chelates with transition metals to be more stable, and thus the oxidation–reduction reaction slows down (Pathak et al., 2020). MAA moieties in the hydrogels also bear carboxylic acid functionality (pKa = 4.88) and lack additional hydroxyl groups. Although hydroxyl groups may be provided by adjacent pHEMA chains, strong binding of Au^{3+} to the carboxylic acid groups may explain why AuNPs formation was not evident at room temperature in the time frame of 72 h for hydrogels H and B. In the case of 1-Day Acuvue® Moist® with Lacreon® the reductant capability at room temperature can be clearly attributed to the embedded PVP and not to the network (as further demonstrated below) (Xan et al., 2010).

Differently to MAA, AMPSA bears a sulfonic acid of lower pKa 1.67 (ChemicalBook.com, 2023). No reports on the use of AMPSA as reducing agent were found. Amidosulfonic acid, which shares the sulfonic acid in common with AMPSA, has been found to act as leaching agent during reduction of transition metals by glucose (Wang et al., 2019). Sulfonic acids may perform more like inorganic acids and only interact with metal ions through hydrogen bonds; thus, differently to carboxylic acids, sulfonic acids do not form chelates (Okonkwo et al., 2021). This may explain the lower binding of gold ions to the hydrogels made with AMPSA (Fig. 2).

Hydrogels prepared with amino-based monomers, AE2 and AE3, were able to sorb most gold ions in solution at room temperature but did not induce apparent reduction. This behavior contrasted with previous reports on the use of polyamino copolymers, such as polyethyleneimine (PEI), and amine-terminated dendrimers which have shown reducing ability at room temperature through a variety of mechanisms (Kuo et al., 2005; Zhang et al., 2008a, 2008b; Zhang et al., 2013).

Silicone hydrogel discs solely or bearing MAA moieties were the only ones that triggered AuNPs formation inside the network since the first hours of incubation at room temperature. Although the information on the use of siloxane polymers as reducing agents is limited, there are some examples of their efficiency in the reduction of citronellal and phosphine oxides though in the presence of catalysts (O'Brien and Wichtand, 2008; Li et al., 2012). Information on metal ions reduction is scarce and attributed to copolymers grafted to the siloxane structure (Racles et al., 2010) or to the curing agent (hardener) of polydimethylsiloxane (Goyal et al., 2009; Zhang et al., 2008a, 2008b). Interestingly, commercially available silicone hydrogel CLs (Unisil and Acuvue® Oasys) behaved similarly, and since the common component is the silicone macromer, the reductive capability could be attributed to the Si moiety in the silane and siloxane monomers (Larson and Fry, 2010). The exception recorded for Biofinity Energys™ silicone hydrogels is likely due to the relative high content in fluorine in the neighborhood of Si. Fluorine is a strong oxidant since it is the most electronegative element. Thus, fluorine did not prevent from the uptake of gold ions but hindered the reduction inside the silicone hydrogel.

3.2. X-ray spectra and SEM images

Steam heat sterilized AuNPs-containing hydrogels were washed for one week, freeze-dried, and the crystallinity of AuNPs investigated. X-ray spectra of the hydrogels evidenced the amorphous state of the polymer network, with broad bands in the 20–30 °2θ range, and three crystalline peaks at 38.078 (intense), 44.256 and 64.376 °2θ (Fig. 4 **A**). These peaks are typical of Au face center cubic lattice nanocrystals (Jung et al., 2022) and thus confirmed that pure AuNPs were formed inside the cross-linked networks. SEM images evidenced that the AuNPs were highly anisotropic showing heterogeneous sizes and shapes, with a predominance of truncate triangle and hexagonal plates (Fig. 4 **B-G**). Silicone hydrogels S1 contained the highest density in AuNPs and also larger particles, which clearly corroborated with the greater relative intensity of the Au peaks in the X-ray spectra (Fig. 4 **A**). Mixtures of small and large anisotropic AuNPs have been reported when extracts of natural plants were used for gold reduction at acid pH and room temperature, while heating of the extract-gold precursor mixture at 100 °C caused rapid formation of small spherical particles (Krishnamurthy et al., 2010; Krishnamurthy et al., 2014). Differently to those previous findings, the developed hydrogels facilitated by themselves the formation of anisotropic AuNPs and the steam heat sterilization favored the process providing in few minutes large particles, which many be particularly useful for in the red light-near infrared applications. Even for Biofinity Energys™ silicone CLs which did not reduce gold ions at

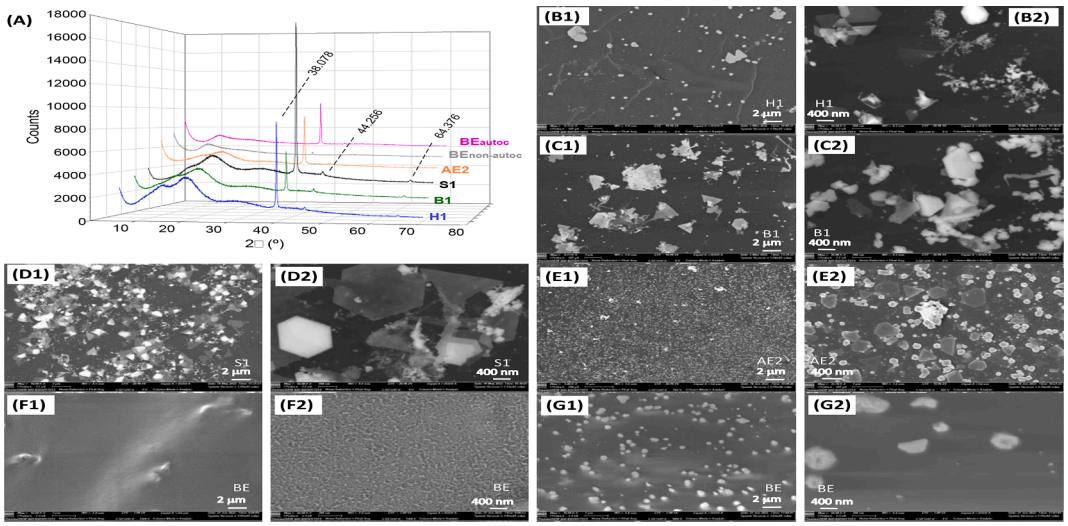

Fig. 4. (A) X-ray spectra and (B-E) SEM images of hydrogels after soaking in $HAuCl_4$ solution (0.327 mM, 2 mL) for 72 h, subsequent steam heat sterilization (autoclave, 121 °C, 20 min), and freeze-drying. Biofinity Energys™ (BE) silicone hydrogels were also analyzed after one month storage in the $HAuCl_4$ solution and before autoclaving (grey line). For visualization purposes, counts of X-ray spectra were progressively shifted 1,000 counts upward from sample to sample. SEM images were acquired at two magnifications (10,000x and 50,000x) for (B1, B2) H1 hydrogels, (C1, C2) B1 hydrogels, (D1, D2) S1 hydrogels, (E1, E2) AE2 hydrogels, (F1, F2) BE hydrogels before autoclaving, and (G1, G2) BE hydrogels after autoclaving.

room temperature even after weeks of storage (Fig. 4 **A**), steam heat sterilization of gold-ion soaked CLs triggered the formation of anisotropic AuNPs, although at much lesser extent than for the other hydrogel compositions tested. Mean circularity values calculated using ImageJ were 0.745 for H1 (138 particles), 0.654 for B1 (60 particles), 0.704 for S1 (60 particles), and 0.831 for Biofinity Energys™ (16 particles).

3.3. Content in water

One concern associated to the loading of AuNPs inside CLs during polymerization or using strong inorganic reductants is related to the significant decrease in water content of the hydrogels (Salih et al., 2021), which may compromise their biomedical applications. In particular, water content plays a key role in ocular comfort during CL wearing and is critical for oxygen diffusion in the case of soft CLs. Relevantly, the protocol developed by us of incubation in the $HAuCl_4$ solution (0.327 mM, 2 mL) for 3 days and subsequent sterilization did not cause detrimental effects on the content in water (Fig. 5). The values recorded for H, S, B and AE hydrogels were in good agreement with those previously reported for related hydrogels (Pereira-da-Mota et al., 2021). Also, the content in water obtained for the commercial CLs agreed well with the nominal content in water of Esencia® 50, Unisil, Biofinity® Energys™, Acuvue® Oasys and Acuvue® Moist®, which are 50 %, 62 %, 40 %, 38 %, and 58 %, respectively (Garcia del Valle et al., 2021; Contamac Unisil, 2022; CooperVision, 2023; Acuvue, 2022).

3.4. Kinetics of AuNPs formation at room temperature

Since silicone hydrogels S1, S2 and S3 evidenced great reductive ability, the next step was to investigate the kinetics of AuNPs formation by recording the changes in transmittance of the hydrogels over time in the absence of light and heating (20 °C constant temperature). To avoid concerns about DMSO traces that may promote transition metals reduction (Patakfalvi et al., 2008), a new batch of silicone hydrogels (S1b, S2b, S3b) was prepared with MAA but without DMSO. DMSO was needed as cosolvent when AMPSA was used, but it was not required for MAA. This new batch showed homogeneous red–purple staining in few hours. The color was faint in the first three days of incubation. Half replicates (n = 3) were autoclaved after 3 days incubation in $HAuCl_4$ solution (0.327 mM, 2 mL) (Fig. 6**A**) to serve as positive controls of the maximum reducing capability. As observed above for other silicone hydrogels, steam heat sterilization caused an immediate decrease in transmittance in the 500–600 nm region, and prolonged incubation in the same gold solution after autoclaving only caused minor further decrease in the transmittance. This suggests that a maximum in gold conversion was reached during autoclaving, which did not increase during extended storage in $HAuCl_4$ solution. Interestingly, a shift in the transmittance peak from 550 to 570 nm (redder wavelengths) was observed as the content in MAA in the silicone hydrogels increased (Fig. 6**A**). Indeed, according to the minima in transmittance recorded, autoclaved S3b hydrogels led to less but larger nanoparticles (Haiss et al., 2007). Overall, autoclaving was shown to be a simple and very

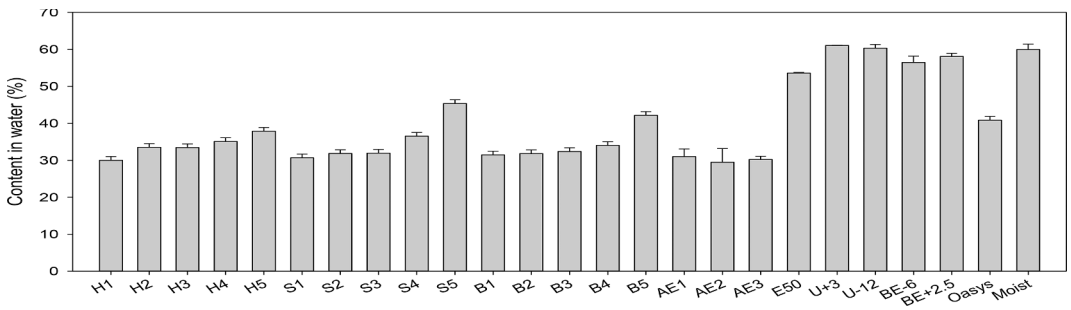

Fig. 5. Water content of swollen discs and CLs measured after 3 days incubation in the $HAuCl_4$ solution (0.327 mM, 2 mL) and subsequent sterilization, referred to the total weight of the wet network. Mean values and standard deviations (n = 3).

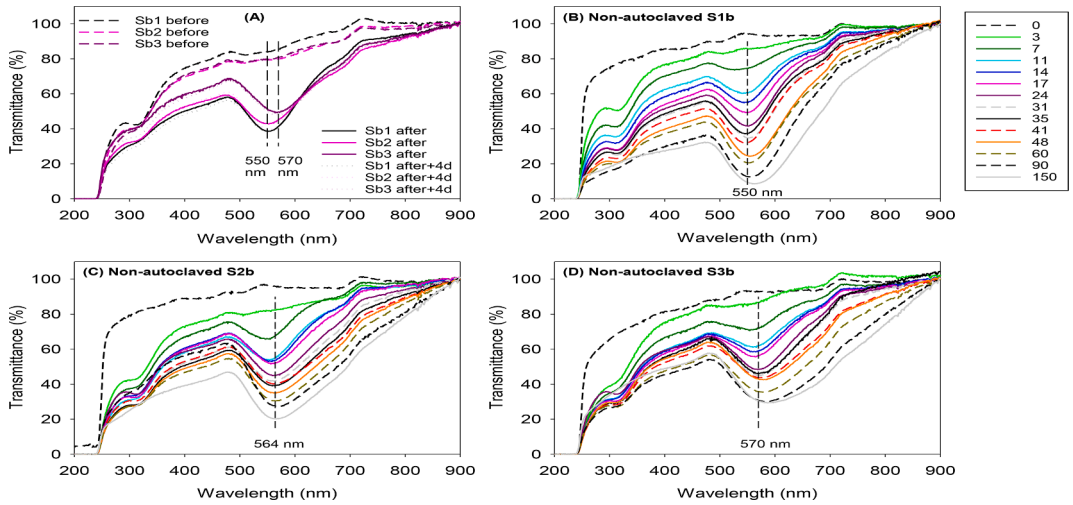

Fig. 6. (A) Transmittance of S1b, S2b and S3b discs that were incubated in $HAuCl_4$ solution (0.327 mM, 2 mL) for 72 h (code "before") and then steam heat sterilized (autoclave, 121 °C, 20 min) (code "after"); sterilized discs were stored at room temperature protected from light during 4 days more and then the transmittance recorded again. (B, C, D) Evolution of the transmittance patterns of S1b, S2b and S3b discs during incubation in $HAuCl_4$ solution (0.327 mM, 2 mL) in water at room temperature protected from light for five months. Transmittance values at time 0 refer to the transmittance recorded for dried discs immediately before immersion in the gold solution. The legend refers to incubation days.

efficient method to produce anisotropic AuNPs inside CL using much lower concentrations of gold ions than when using inorganic catalysts, which furthermore only generate spherical particles (Liu and Chauhan, 2022; Liu et al., 2021). After autoclaving, remarkably low transmittances in the 550–570 nm interval were achieved: 38 % transmittance for silicone hydrogels without MAA and 50 % transmittance for silicone hydrogels with MAA, while still allowing vision through them. Moreover, the obtained light blocking capability was in the range reported for HEMA-based CLs synthesized in the presence of preformed AuNPs of 40–80 nm size (Salih et al., 2021) or with much larger (~500 nm) gold nanocapsules (Mariño-López et al., 2019) while avoiding the need of modifying the CLs synthesis protocols.

Images of a rainbow with the main seven colors printed as equally wide strips were taken with the autoclaved and non-autoclaved S1b, S2b and S3b hydrogels placed on the objective of a mobile phone camera (**Figure S3 Supporting Information**). Compared to the control (no hydrogel; **Figure S3 D**), hydrogels containing AuNPs slightly attenuated the colors, but all colors and particularly the white strip on the left of the rainbow became more violet or magenta. Violet is the complementary color of yellow, with dominant wavelength in the 575–585 nm range. In the RGB scale, violet is represented by code #5F2879 and consists of 37.3 % red, 15.7 % green and 47.5 % blue. Green has the main wavelength in the 495–570 nm range and red in the 620–750 nm range. These findings are in good agreement with the transmittance spectra recorded for the hydrogels (Fig. 6).

Replicates that did not undergo autoclaving (n = 3) but remained stored at room temperature evidenced progressive decrease in the transmittance in the 500–700 nm region (Fig. 6 **B-D** and Fig. 7**A**), which was shown as a remarkable increase in the red–purple staining. The peak in transmittance was monitored along time at 550, 564 and 570 nm for

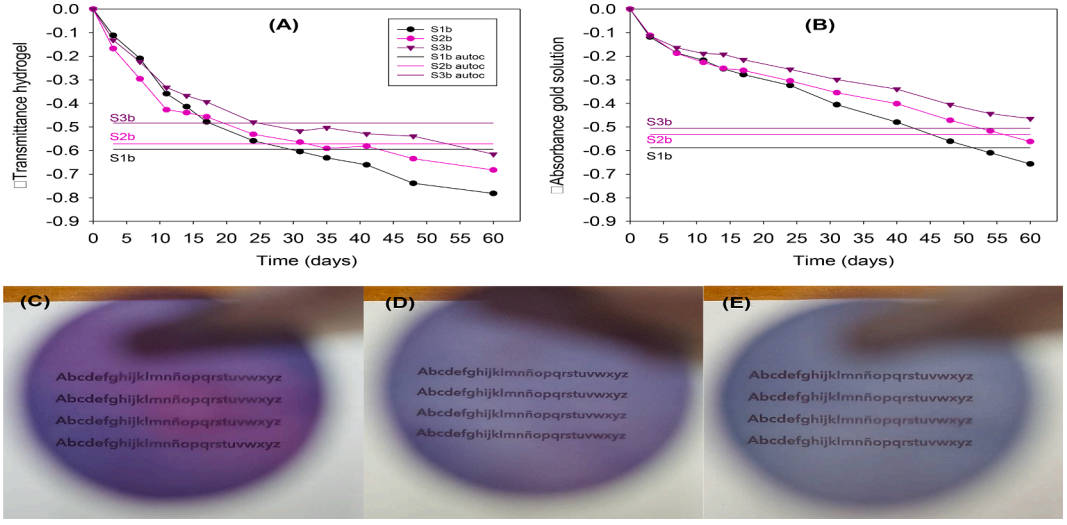

Fig. 7. (A) Relative decrease in transmittance of S1b, S2b and S3b discs at 550, 564 and 570 nm, respectively, during incubation in $HAuCl_4$ solution (0.327 mM, 2 mL) at room temperature protected from light for two months. Continuous lines (parallel to X-axis) represent the minimum transmittance values recorded at 550, 564 and 570 nm for S1b (no MAA), S2b (100 mM MAA) and S3b (200 mM MAA) after being autoclaved. (B) Relative decrease in the absorbance of the $HAuCl_4$ solution in the presence of S1b, S2b and S3b discs. Continuous lines (parallel to X-axis) represent the minimum absorbance value at 287 nm recorded for S1b, S2b and S3b after being autoclaved. (C, D, E) Images taken by placing S1b, S2b and S3b discs, respectively, between the lens of a mobile phone and a text. The wet discs were removed from the $HAuCl_4$ solution after five months storage and carefully placed at a distance of 5 cm from the camara lens.

S1b (no MAA), S2b (100 mM MAA) and S3b (200 mM MAA) and referred to the transmittance of each disc before immersion in the $HAuCl_4$ solution, as follows.

$$\Delta Transmittance = \frac{Tf - Ti}{Ti} \quad (2)$$

In this equation, *Tf* represents the transmittance value recorded at time *t* after incubation in the $HAuCl_4$ solution, and *Ti* refers to the transmittance of each disc before immersion. As depicted in Fig. 7 **(A)**, the transmittance decayed almost linearly along time in the first two weeks and then the rate decreased. It took approx. 30 days of incubation to the hydrogels at 20 °C to reach the same decay in transmittance as shown by the autoclaved hydrogels (121 °C, 15 min). A strong dependence of the seed growth process on temperature was previously found when using citrate as reducing agent; the time required for a significant mean size increase was reported to be 15 min at 100 °C (Agunloye et al., 2018). According to that, the conventional CL sterilization protocol by autoclaving generated the best conditions for the silicone hydrogel network to fully develop its properties as reductant agent in an accelerated manner. Nevertheless, the minimum in transmittance that was recorded after 60 days of incubation at room temperature (20 %, 30 % and 35 % for S1b, S2b, and S3b, respectively) was somehow below of that recorded after autoclaving, which indicated that the CL network may provide an adequate environment for the complete reduction of the gold ions at room temperature if time is given. It can be hypothesized that in the polymer network the concentration in reducing agents was in excess compared to the initial concentration of $HAuCl_4$. In this regard, the slow drop in absorbance at 287 nm of the external gold solution (Fig. 7**B**) suggested more efficient reduction of gold and growth of AuNPs inside the hydrogel at 20 °C than during autoclaving; i.e., the same drop in transmittance of the CL was achieved with less consumption of gold ions. Namely, the hydrogels incubated at room temperature required more time but less gold ions to block the light the same as the autoclaved ones. As mentioned above, at 20 °C the hydrogels took 30 days in blocking the same percentage of light as the autoclaved hydrogels but had consumed approx. half of gold ions. Probably, the intense heating of the steam heat sterilization generated more seeds of lower size with an increased consumption of gold ions. It should be noted that the acid conditions (pH 3) of the medium have been shown to favor the seeding process too (Agunloye et al., 2018).

After 5 months storage, S1b, S2b, and S3b had sorbed ca. 100 % gold ions from the medium and the transmittance at 550, 564 and 570 nm was of 9.3, 20.2, and 30.1 % respectively (Fig. 6 **B,C,D**). The slow AuNPs formation at 20 °C allowed for a precise control of the percentage of gold reduction or of light blocking since the reaction stopped when the hydrogels were transferred to water. Soaking in water removed the free gold ions and preserved the decrease in transmittance of the hydrogels in the desired region, without leakage of AuNPs to the aqueous medium. Relevantly for the practical use as CLs, the strong blocking of the transmittance in the 500–700 nm region attained after 5 months storage (**Figure S4 in Supporting Information**) still allowed seeing through the hydrogels with high sharpness (Fig. 7 **C-E**).

Also remarkably, the shift in the decrease of transmittance peak towards redder wavelengths was clearly seen for S3b hydrogels (which were more violet-blueish). This finding suggests that while silicone hydrogel itself triggers the formation of AuNPs, MAA may facilitate the nucleation and growth of larger particles (greater than100 nm) (Haiss et al., 2007). Poly(acrylic acid) (PAA) nanogels have previously been explored to prepare Au irregular clusters that absorbed in the NIR region but using cysteamine as gold chelating agent and $NaBH_4$ as reduction agent (Chen et al., 2014). Reports on reduction by acrylic acid derivatives in the absence of inorganic reducing agents are very limited. Sodium alginate with grafted chains of dimethylacrylamide and acrylic acid was shown to act as gold reducing and encapsulating agent when incubated with $HAuCl_4$ at 90 °C and pH 8 (Kolya et al., 2015). Although the temperature and pH conditions tested were well above those explored in our study, shifts in the UV–Vis absorption spectra towards higher wavelengths (from 530 to 573) were observed when the processing time of copolymer graft-gold dispersion at 90 °C was prolonged from 3 to 20 min. In this line, PAA brushes bearing silver nanoparticles have been shown able to induce the growth of gold octahedra superstructures (~500 nm) in the presence of cetyltrimethylammonium bromide (CTAB), which guided the growth of specific crystal faces (Wang et al., 2015). Once again, the role of PAA itself was overlooked in the previous papers.

3.5. Reaction in NaCl 0.9 % medium

Since CLs are commonly commercialized and stored in NaCl 0.9 % (154 mM) medium, which mimics the osmotic pressure of lachrymal fluid as well as interstitial water, next experiments were devoted to gain an insight into the effect of NaCl on the AuNPs formation process. Dried S1b, S2b and S3b silicone hydrogel discs and Acuvue® Oasys with HydraLuxe™ and 1-Day Acuvue® Moist® with Lacreon® CLs directly removed from the original blisters were incubated in 0.327 mM $HAuCl_4$ solution prepared in NaCl 0.9 % (2 mL). Since these commercial CLs are quite thin, they were not previously washed or dried to avoid conformational changes and distortion of the structure. Nevertheless, we observed that while the small aliquots of CL storage liquid (0.2 mL in 2 mL 0.327 mM $HAuCl_4$ solution) did not induce the reduction of gold ions at room temperature, the mixtures of storage liquid and gold precursor solution became pale pink (Acuvue® Oasys with HydraLuxe™) and reddish (1-Day Acuvue® Moist® with Lacreon®) after autoclaving both when the $HAuCl_4$ solution was prepared in water and in NaCl 0.9 %. Also greater storage liquid:$HAuCl_4$ solution v/v mixtures (1:1) slowly triggered AuNPs formation at room temperature in the case of 1-Day Acuvue® Moist® with Lacreon® CLs. TEM images confirmed the formation of AuNPs (**Figure S5 in Supporting Information**) after autoclaving; AuNPs were larger and clearly anisotropic in the medium of the 1-Day Acuvue® Moist® with Lacreon® storage liquid, which can be attributed to the presence of PVP. Thus, in the case of commercially available CLs, the role of maintenance liquids as reductant agents must be considered.

The UV–vis spectrum of $HAuCl_4$ solution prepared in NaCl 0.9 % was quite different from that recorded in water in the absence of the salt. The maximum of absorption shifted from 287 to 308 nm (**Figure S1**). After 3 days storage, the absorbance of the gold solution and the light transmittance of the discs were monitored as reported above (Fig. 8 and **Figure S6** in **Supporting Information**). In the NaCl 0.9 % medium, the hydrogels loaded similar or even greater amounts of gold from the solution (Fig. 8**A**) than when the process was carried out in pure water (Fig. 2**E and 3E**). However, unexpectedly, S1b, S2b and S3b silicone hydrogels failed to reduce gold in the presence of NaCl 0.9 % (Fig. 8**B**, and **Figure S6 A1, B1 and C1**). After 3 days incubation, a strong decrease in transmittance was recorded in the region corresponding to the absorbance of $HAuCl_4$ solution prepared in NaCl 0.9 %, which indicated that the hydrogels strongly absorbed gold ions. Nevertheless, the hydrogels maintained the colorless appearance. When autoclaving was applied, no changes in the transmittance pattern were observed, revealing that gold reduction did not take place. Some replicates were not autoclaved, but intensively washed in water for 5 days and then transferred to $HAuCl_4$ solution prepared in water in order to check whether the capability to reduce gold could be recovered in the absence of NaCl. The absorbance of the gold solution and the transmittance of the discs were recorded again at different time points during storage (**Figure S6 A2, B2 and C2**). The decays in hydrogels transmittance (**Figure S4 A**) and in the absorbance of the external $HAuCl_4$ aq. solution (**Figure S4 B**) were quite similar to the patterns recorded for S1b, S2b and S3b silicone hydrogels directly immersed in the $HAuCl_4$ solution prepared in water (Fig. 7). This finding clearly pointed out to a specific effect of NaCl on the gold reducing reaction inside the hydrogels.

Acuvue® Oasys with HydraLuxe™ CLs (Fig. 8 **C**) performed

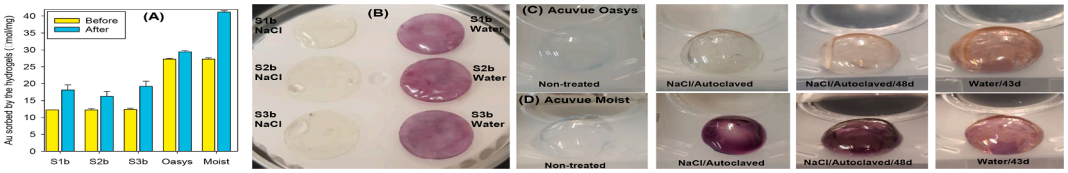

Fig. 8. (A) Amount of gold sorbed by the hydrogels incubated for 3 days at 20 °C in $HAuCl_4$ (0.327 mM, 2 mL) solution prepared in NaCl 0.9 %, before and after autoclaving; mean values and standard deviation (n = 3). (B) On the left, appearance of S1b, S2b and S3b discs incubated for 3 days at 20 °C in $HAuCl_4$ (0.327 mM, 2 mL) solution prepared in NaCl 0.9 % and then autoclaved. On the right, replicates incubated for 3 days at 20 °C in $HAuCl_4$ (0.327 mM, 2 mL) solution prepared in NaCl 0.9 % were then washed with water for 5 days and transferred to $HAuCl_4$ (0.327 mM, 2 mL) solution prepared in water and kept at 20 °C; the picture was taken on day 43 of incubation at 20 °C in $HAuCl_4$ (0.327 mM, 2 mL) solution prepared in water. (C, D) Appearance of Acuvue® Oasys and Acuvue® Moist® CLs as freshly removed from the package (non-treated); CLs after 3 days incubation at 20 °C in $HAuCl_4$ (0.327 mM, 2 mL) solution prepared in NaCl 0.9 % and then autoclaved (NaCl/autoclaved); CLs that remained in the autoclaved $HAuCl_4$ solution prepared in NaCl 0.9 % for 48 days (NaCl/autoclaved/48d); and CLs that were incubated for 3 days at 20 °C in $HAuCl_4$ (0.327 mM, 2 mL) solution prepared in NaCl 0.9 %, then washed with water for 5 days, and finally transferred to $HAuCl_4$ (0.327 mM, 2 mL) solution prepared in water and kept at 20 °C; the picture was taken on day 43 of incubation at 20 °C in $HAuCl_4$ (0.327 mM, 2 mL) solution prepared in water.

similarly to the silicone hydrogels discs and the changes in transmittance were minor both before and after autoclaving in $HAuCl_4$ solution prepared in NaCl 0.9 % (**Figure S6 D**). They recovered the capability to reduce gold once transferred to solutions prepared in water. In the case of 1-Day Acuvue® Moist® with Lacreon® CLs the behavior was completely different; the CLs autoclaved in $HAuCl_4$ solution prepared in NaCl 0.9 % acquired an intense cherry-like color (Fig. 8 **D**), with a strong decrease in transmittance in the 500–600 nm region (**Figure S6 E**). This strong reductant capability can be assigned to the PVP embedded into the CL and not to the CL network itself (as evidenced in the TEM images). Replicates of Acuvue® Moist® CLs transferred to water medium before autoclaving performed as observed previously in the absence of NaCl (**Figure 6 D1**).

The effect of NaCl on gold reduction using organic reductant agents has barely been investigated, and most information available refers to NaCl concentrations well below the physiological one (e.g., three orders of magnitude), which triggered minor changes in AuNPs formation (Krishnamurthy et al., 2010). Li et al. (2021b) observed that cross-linked amide-functionalized polydopamine, chitosan and cellulose hydrogels decreased their capability to reduce gold when NaCl concentration increased from 0.1 to 1.0 M, which was attributed to lower adsorption capability of the polymers due to conformational changes at high ionic strengths. Conformational changes may have happened too in the silicone hydrogels although, apparently, they did not compromise the capability of the hydrogels to adsorb gold ions (as shown by the high amount of gold ions entrapped; Fig. 8**A**). Xu et al. (2014) found that the rate of reduction of silver by PVP slowed down by increasing the ratio of NaCl. Also, when NaCl concentration was high (Ag^+:Cl^- 1:3 mol ratio) one-dimensional silver nanorods were obtained instead of microparticles. These effects were attributed to that an excess of Cl^- might alter the reduction equilibrium towards the ionic species and also causes changes in the solubility of partially reduced species. In our case, the $HAuCl_4$:NaCl mol ratio was of 1:470. Thus, NaCl was clearly in excess compared to $HAuCl_4$, and both changes in the conformation of the reductant moieties in the hydrogel and of the gold species may have occurred. The increase in pH from 3.0 to 3.5 caused by NaCl was quite small to alter the catalytic activity of the protons. In any case, the conformational changes in the silicone hydrogel, if any, were reversible, and the CLs recovered their functionality as reductant agents when transferred to water medium.

To gain a further insight into the light absorption features of the S1b, S2b and S3b silicone hydrogel discs, the spectra were recorded in the 200–2000 nm range using a V-770 UV–Visible/NIR spectrophotometer (Jasco, Japan) against a baseline recorded in air. The spectra (**Figure S7 in Supporting Information**) confirmed the high light transmission of the hydrogels before any treatment and evidenced a decrease in transmittance of AuNPs-containing hydrogels from 500 nm toward the red region that expanded in the near-infrared region. No relevant differences were recorded between discs that were previously exposed or not to the NaCl 0.9 % solution, confirming the capability of the silicone hydrogels to reduce gold in water and produce anisotropic particles in the absence of any other reagent.

3.6. *Responsiveness to laser light*

Photothermal responsiveness of the wet discs with and without AuNPs was evaluated using 100 mW laser pointers: namely, a 532 nm green laser and a 652 nm red laser (both with beam diameter of 2.0 mm) and a 808 nm near-infrared laser (beam diameter 3.0 mm). Illuminance of the lasers was previously recorded with the lasers placed at a vertical distance of 19 cm with respect to a power meter sensor. Then, discs were placed (one each time) on the power meter sensor to be irradiated with the laser pointers. This set-up allowed simultaneous recording of both blockage of the illuminance and changes in temperature of the discs (by means of a thermographic camera) (Fig. 9, and **Figures S8 and S9** for green laser and **Figures S11 and S12** for NIR laser in **Supporting Information**). Non-treated discs (without AuNPs) did not change either illuminance or temperature after 10 s irradiation with any laser pointer in good agreement with their transmittance spectra. Also, the power meter sensor did not change its temperature after 10 s irradiation with any of the lasers.

Discs that were prepared by soaking in $HAuCl_4$ solution (0.327 mM, 2 mL) for 72 h, subsequent steam heat sterilization (autoclave, 121 °C, 20 min), and then storage in water for 6 months increased 10 to 25 °C their temperature when irradiated with the green laser for 10 s. These discs blocked 20–70 % of light radiation depending on the hydrogel composition (**Figure S10** in **Supporting Information**). As expected from **Figure 2, S1** hydrogels incubated for 3 days in $HAuCl_4$ and then steam heat sterilized, which were the most efficient ones in terms of gold reductant capability, showed the greatest light blockage capability. These same discs also showed photothermal performance when irradiated with the NIR 808 nm laser, although with smaller increases in temperature ranging from 7 to 16 °C and light blockage of 30–50 % (**Figure S10** in **Supporting Information**).

S1b, S2b and S3b silicone hydrogel discs that were incubated in $HAuCl_4$ (0.327 mM, 2 mL) solution prepared in water and kept at 20 °C for 143 days were the most efficient ones in terms of both photothermal effect and radiation blockage (Fig. 9). When the hydrogels were irradiated with the 532 nm laser the temperature increased 45–65 °C in 10 s and decreased the illumination up to 37.5 %. Such an increase in temperature was in good agreement with the findings previously reported by Liu and Chauhan (2022) for AuNPs-containing Acuvue® Moist® and TrueEye® contact lenses prepared by soaking in the gold precursor and subsequent immersion in a strong sodium borohydride reductant solution. Such a high efficiency in radiation absorption has been attributed to the large size of the nanoparticles formed, although it may also depend on the concentration of AuNPs and the thermal conductivity of the polymer network.

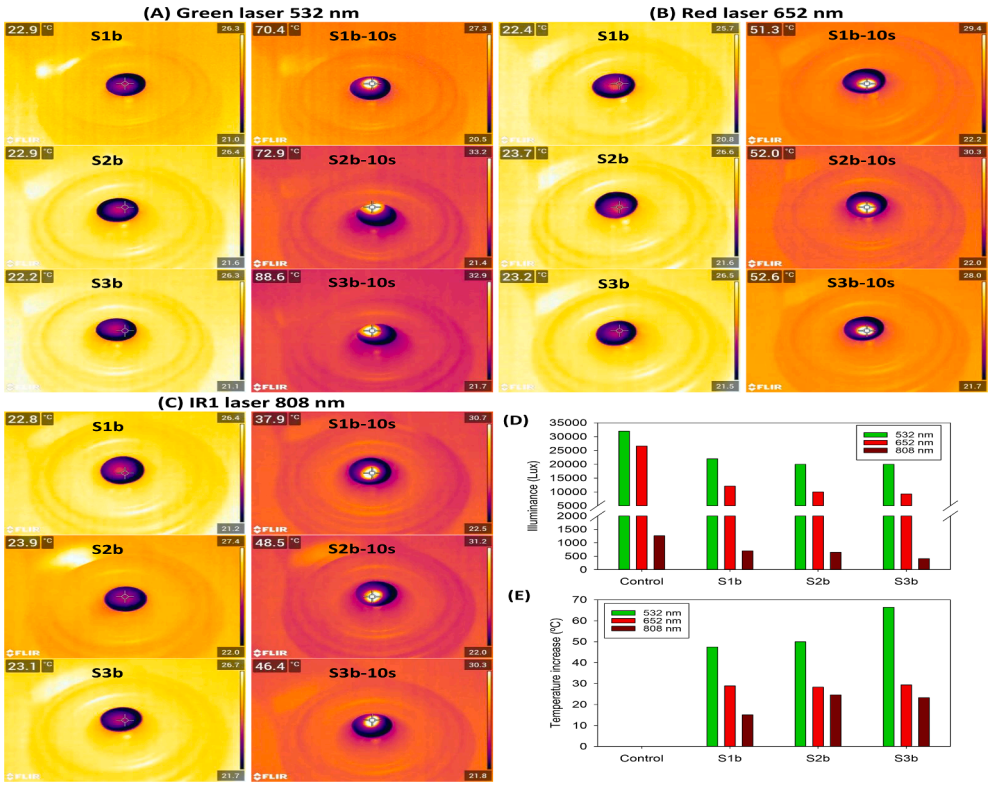

Fig. 9. (A-C) Thermal images of wet discs before and after 10 s irradiation with green, red or NIR laser (100 mW), (D) laser light attenuation recorded during laser exposition, and (E) increase in temperature of the discs after 10 s irradiation. These hydrogels were obtained by incubation for 3 days at 20 °C in $HAuCl_4$ (0.327 mM, 2 mL) solution prepared in NaCl 0.9 %, then washed with water for 5 days and transferred to $HAuCl_4$ (0.327 mM, 2 mL) solution prepared in water and kept at 20 °C for 143 days. (For interpretation of the references to color in this figure legend, the reader is referred to the web version of this article.)

Since AuNPs-containing S1b, S2b and S3b silicone hydrogel discs also showed relevant decrease in the transmittance of higher wavelength light (**Figure S7** in **Supporting Information**), their performance under red (652 nm) and near-infrared (808 nm) radiation was also investigated. Exposition to red laser caused an increase in temperature of 28–29 °C and the illumination decreased 55–65 %, while exposition to near-infrared laser increased the temperature 15–25 °C and the illumination decreased 45–65 % (Fig. 9). These results evidenced the suitability of the polymer-triggered gold reduction to prepare hydrogels with the capability to absorb radiation in the near-infrared physiological window, which may open a wide range of therapeutic applications. Applications of these polymers may be envisioned both as protection of inner eye structures (blockage of light) but also as well-controlled confined photothermal therapy tools against eye tumors on the anterior segment (Luo et al., 2015) or for prevention and management of posterior capsule opacification associated to intraocular lenses (Lin et al., 2017). For example, for this latter application, Au@SiO_2 nanorods (82 ± 8 nm in length and 46 ± 3 nm in width) were grafted to the IOL and when irradiated with 808 nm laser (2 W/cm^2) the temperature increased 15.2–27.6 °C after 80 s irradiation. The AuNPs-containing hydrogels developed by us can provide similar temperature increase in 10 s. Such an effective photothermal response in such a short time may pave the way for clinical translation as the patient would have to avoid blinking for only 10 s.

4. Conclusions

Hydrogels commonly used as CLs can readily uptake in a few hours gold ions from water, which can be transformed in anisotropic AuNPs by means of common wet sterilization protocols. This strategy appears as a general protocol that can be applied to any hydrogel network disregarding its monomeric composition and in the absence of any other reagent. This protocol is fast and AuNPs formation does not proceed further when the hydrogel is cooled down. Relevantly, hydrogels prepared with silicone monomers exhibit intrinsic reductive ability to transform gold ions into anisotropic AuNPs at room temperature in the absence of light and any other source of energy. This alternative protocol proceeds at a slow rate, which makes it possible to stop the reaction once a desired content in AuNPs is achieved. Importantly, monomers bearing F atoms efficiently hindered the capability of the hydrogels to reduce gold ions at room temperature and therefore, hydrogels containing F moieties produce less AuNPs and only when steam heated. The AuNPs-containing CLs can be stored for months in water or NaCl 0.9 % solution without leakage of the AuNPs.

Silicone hydrogels prepared with MAA comonomers showed a shift in the absorbance towards reddish, which endows them with greater capability of absorption of red and near-infrared radiation, which in turn can be useful both for attenuating the light entering the eye and for a very localized increase in temperature in the ocular tissues. The simplicity of the developed protocol for generating anisotropic AuNPs into hydrogels that still preserve their wettability and can be stored for months in aqueous medium without changes in the transmittance spectrum and photothermal responsiveness may open a wide range of novel applications in therapy and diagnosis.

CRediT authorship contribution statement

Carmen Alvarez-Lorenzo: Conceptualization, Data curation, Formal analysis, Funding acquisition, Investigation, Methodology, Project administration, Resources, Software, Supervision, Validation, Visualization, Writing – original draft, Writing – review & editing. **Maria Vivero-Lopez:** Data curation, Formal analysis, Methodology, Software, Validation, Writing – review & editing. **Angel Concheiro:** Conceptualization, Formal analysis, Funding acquisition, Investigation, Methodology, Project administration, Resources, Supervision, Writing – original draft, Writing – review & editing.

Declaration of Competing Interest

The authors declare the following financial interests/personal

relationships which may be considered as potential competing interests: Carmen Alvarez-Lorenzo reports equipment, drugs, or supplies was provided by Spain Ministry of Science and Innovation. Carmen Alvarez-Lorenzo reports equipment, drugs, or supplies was provided by Government of Galicia Department of Culture Education and Universities. Carmen Alvarez-Lorenzo reports equipment, drugs, or supplies was provided by European Regional Development Fund. Carmen Alvarez-Lorenzo has patent #Patent EP23382049.7 Gold Nanoparticle Hydrogels pending to Universidade de Santiago de Compostela. Angel Concheiro has patent #Patent EP23382049.7 Gold Nanoparticle Hydrogels pending to Universidade de Santiago de Compostela.

Data availability

Data will be made available on request.

Acknowledgment

The authors would like to thank the use of RIAIDT-USC analytical facilities.

Funding

The work was supported by MCIN [PID 2020-113881RB-I00/AEI/10.13039/501100011033], Spain, FEDER and Xunta de Galicia [ED431C 2020/17].

Author Contributions

The manuscript was written through contributions of all authors. All authors have given approval to the final version of the manuscript.

Appendix A. Supplementary material

Supplementary data to this article can be found online at https://doi.org/10.1016/j.ijpharm.2023.123048.

References

Acuvue Technical Specifications. https://www.acuvue.com/sites/acuvue_us/files/products-spec-sheet.pdf, July 2022.

Agunloye, E., Panariello, L., Gavriilidis, A., Mazzei, L., 2018. A model for the formation of gold nanoparticles in the citrate synthesis method. Chem. Engin. Sci. 191, 318–331. https://doi.org/10.1016/j.ces.2018.06.046.

Alvarez-Lorenzo, C., Mayo-Olveira, F., Barbosa, S., Taboada, P., Concheiro, A., 2020. Poly(vinyl alcohol) triggers Au nanoparticles formation for NIR-responsive gels and nanofibers. J. Appl. Polym. Sci. 137, 48811. https://doi.org/10.1002/app.48811.

Beining, M.W., Magnø, M.S., Moschowits, E., Olafsson, J., Vehof, J., Dartt, D.A., Utheim, T.P., 2022. In-office thermal systems for the treatment of dry eye disease. Survey Ophthalmol. 67, 1405–1418. https://doi.org/10.1016/j.survophthal.2022.02.007.

Bhavsar, K.V., Michel, Z., Greenwald, M., Cunningham, E.T., Freund, K.B., 2021. Retinal injury from handheld lasers: A Review. Survey Ophthalmol. 66, 231–260. https://doi.org/10.1016/j.survophthal.2020.06.006.

Cabana, S., Lecona-Vargas, C.S., Melendez-Ortiz, H.I., Contreras-Garcia, A., Barbosa, S., Taboada, P., Magarinos, B., Bucio, E., Concheiro, A., Alvarez-Lorenzo, C., 2017. Silicone rubber films functionalized with poly(acrylic acid) nanobrushes for immobilization of gold nanoparticles and photothermal therapy. J. Drug Deliv. Sci. Technol. 42, 245–254. https://doi.org/10.1016/j.jddst.2017.04.006.

Cabana-Montenegro, S., Barbosa, S., Taboada, P., Concheiro, A., Alvarez-Lorenzo, C., 2019. Syringeable self-organizing gels that trigger gold nanoparticles formation for localized thermal ablation. Pharmaceutics 11, 52. https://doi.org/10.3390/pharmaceutics11020052.

ChemicalBook. https://www.chemicalbook.com/ChemicalProductProperty_EN_CB3470952.htm; accessed March 2023.

Chen, Y., Zheng, X., Wang, X., Wang, C., Ding, Y., Jiang, X., 2014. Near-infrared emitting gold cluster−poly(acrylic acid) hybrid nanogels. ACS Macro Lett. 3, 74–76. https://doi.org/10.1021/mz4005748.

Cho, Y.C., Kang, J.M., Park, W., Kim, D.H., Shin, J.H., Kim, D.H., Park, J.H., 2021. Photothermal therapy via a gold nanoparticle-coated stent for treating stent-induced granulation tissue formation in the rat esophagus. Sci. Rep. 11, 10558. https://doi.org/10.1038/s41598-021-90182-x.

Contamac Unisil, https://www.contamac.com/product/unisil, July **2022**.

CooperVision. Product Reference Guide. https://coopervision.com/sites/coopervision.com/files/14326-product-reference-guide-3-23-r2.pdf; accessed March **2023**.

Dumur, F., Guerlin, A., Dumas, E., Bertin, D., Gigmes, D., Mayer, C.R., 2011. Controlled spontaneous generation of gold nanoparticles assisted by dual reducing and capping agents. Gold Bull. 44, 119–137. https://doi.org/10.1007/s13404-011-0018-5.

Garcia del Valle, A.M., Blázquez, V., Gros-Otero, J., Infante, M., Culebras, A., Verdejo, A., Sebastián, J., García, M., Bueno, S., Piñero, D.P., 2021. Efficacy and safety of a soft contact lens to control myopia progression. Clin. Exp. Optom. 104, 14–21. https://doi.org/10.1111/cxo.13077.

Goyal, A., Kumar, A., Patra, P.K., Mahendra, S., Tabatabaei, S., Alvarez, P.J.J., John, G., Ajayan, P.M., 2009. In situ synthesis of metal nanoparticle embedded free standing multifunctional PDMS films. Macromol. Rapid Commun. 30, 1116–1122. https://doi.org/10.1002/marc.200900174.

Goy-Lopez, S., Taboada, P., Cambon, A., Juarez, J., Alvarez-Lorenzo, C., Concheiro, A., Mosquera, V., 2010. Modulation of size and shape of Au nanoparticles using amino-X-shaped poly(ethylene oxide)-poly(propylene oxide) block copolymers. J. Phys. Chem. B 114, 66–76. https://doi.org/10.1021/jp908569z.

Haiss, W., Thanh, N.T.K., Aveyard, J., Fernig, D.G., 2007. Determination of size and concentration of gold nanoparticles from UV-Vis spectra. Anal. Chem. 79, 4215–4221. https://doi.org/10.1021/ac0702084.

Jung, Y., Do, T., Choi, U.S., Jung, K.W., Choi, J.W., 2022. cage-like amine-rich polymeric capsule with internal 3D center-radial channels for efficient and selective gold recovery. Chem. Eng. J. 438, 135618 https://doi.org/10.1016/j.cej.2022.135618.

Kapfelsberger, A., Eckstein, J., von Ahrentschild, A., Bischoff, J., Marx, S., Sickenberger, W., 2021. Ultraviolet and visible transmittance of soft contact lenses with and without ultraviolet blockers. Optom. Vis. Sci. 98, 1270–1278. https://doi.org/10.1097/OPX.0000000000001796.

Kolya, H., Pal, S., Pandey, A., Tripathy, T., 2015. Preparation of gold nanoparticles by a novel biodegradable graft copolymer sodium alginate-g-poly (N, N-dimethylacrylamide-co-acrylic acid) with anti micro bacterial application. Eur. Polym. J. 66, 139–148. https://doi.org/10.1016/j.eurpolymj.2015.01.035.

Krishnamurthy, S., Sathishkumar, M., Kim, S., Yun, Y.S., 2010. Counter ions and temperature incorporated tailoring of biogenic gold nanoparticles. Process Biochem. 45, 1450–1458. https://doi.org/10.1016/j.procbio.2010.05.019.

Krishnamurthy, S., Esterle, A., Sharma, N.C., Sahi, S.V., 2014. Yucca-derived synthesis of gold nanomaterial and their catalytic potential. Nanoscale Res. Lett. 9, 627. https://doi.org/10.1186/1556-276X-9-627.

Kuo, P.L., Chen, C.C., Jao, M.W., 2005. Effects of polymer micelles of alkylated polyethylenimines on generation of gold nanoparticles. J. Phys. Chem. B 109, 9445–9450. https://doi.org/10.1021/jp050136p.

Larson, G.L., Fry, J.L. (Eds.), 2010. Ionic and Organometallic-Catalyzed Organosilane Reductions. Wiley.

Li, X.J., Cui, W.R., Jiang, W., Yan, R.H., Liang, R.P., Qiu, J.D., 2021b. Bi-functional natural polymers for highly efficient adsorption and reduction of gold. Chem. Eng. J. 422, 130577 https://doi.org/10.1016/j.cej.2021.130577.

Li, Y., Lu, L.Q., Das, S., Pisiewicz, S., Junge, K., Beller, M., 2012. Highly chemoselective metal-free reduction of phosphine oxides to phosphines. J. Am. Chem. Soc. 134, 18325–18329. https://doi.org/10.1021/ja3069165.

Li, Q., Ma, C., Ma, Y.P., Ma, Y.P., Mao, Y., Meng, Z.L., 2021a. Sustained bimatoprost release using gold nanoparticles laden contact lenses. J. Biomater. Sci. Polym. Ed. 32, 1618–1634. https://doi.org/10.1080/09205063.2021.1927656.

Li, N., Zhao, P.X., Astruc, D., 2014. Anisotropic gold nanoparticles: synthesis, properties, applications, and toxicity. Angew. Chem. Int. Ed 53, 1756–1789. https://doi.org/10.1002/anie.201300441.

Lin, Y.X., Hu, X.F., Zhao, Y., Gao, Y.J., Yang, C., Qiao, S.L., Wang, Y., Yang, P.P., Yan, J., Sui, X.C., Qiao, Z.Y., Li, L.L., Xie, J.B., Zhu, S.Q., Wu, X.C., Li, Y., Wang, L., Wang, H., 2017. Photothermal ring integrated intraocular lens for high efficient eye disease treatment. Adv. Mater. 29, 1701617. https://doi.org/10.1002/adma.201701617.

Link, S., El-Sayed, M.A., 2000. Shape and size dependence of radiative, non-radiative and photothermal properties of gold nanocrystals. Int. Rev. Phys. Chem. 19, 409–453. https://doi.org/10.1080/01442350050034180.

Liu, Z., Chauhan, A., 2022. Gold nanoparticles-loaded contact lenses for laser protection and meibomian gland dysfunction (MGD) dry eye treatment. Colloids Surf. A 635, 128053. https://doi.org/10.1016/j.colsurfa.2021.128053.

Liu, Z., Kompella, U.B., Chauhan, A., 2021. Gold nanoparticle synthesis in contact lenses for drug-less ocular cystinosis treatment. Eur. J. Pharm. Biopharm. 165, 271–278. https://doi.org/10.1016/j.ejpb.2021.05.019.

Luo, L., Nie, C., Du, P., Hongwei, Z., Wei, W., Zhang, M., Ambati, B., Sun, Z., 2015. An efficient near-infrared photothermal therapy agent by using Ag@oxides nanoprisms in for uveal melanoma therapy. Invest. Ophthalmol. Vis. Sci. 56, 1540.

Mariño-López, A., Sousa-Castillo, A., Carbó-Argibay, E., Otero-Espinar, F., Alvarez-Puebla, R.A., Pérez-Lorenzo, M., Correa-Duarte, M.A., 2019. Laser-protective soft contact lenses: keeping an eye on the eye through plasmonics. Appl. Mater. To. 15, 1–5. https://doi.org/10.1016/j.apmt.2018.12.016.

Mariño-López, A., Álvarez-Puebla, R.A., Vaz, B., Correa-Duarte, M.A., Pérez-Lorenzo, M., 2022. SERS optical accumulators as unified nanoplatforms for tear sampling and sensing in soft contact lenses. Nanoscale 14, 7991–7999. https://doi.org/10.1039/D2NR00531J.

Masse, F., Ouellette, M., Lamoureux, G., Boisselier, E., 2019. Gold nanoparticles in ophthalmology. Med. Res. Rev. 39, 302–327. https://doi.org/10.1002/med.21509.

O'Brien, K.E., Wichtand, D.K., 2008. A Greener organic chemistry experiment: reduction of citronellal to citronellol using poly(methylhydro)siloxane. Green Chem. Lett. Rev. 1, 149–154. https://doi.org/10.1080/17518250802512475.

Okonkwo, E.G., Wheatley, G., He, Y., 2021. The role of organic compounds in the recovery of valuable metals from primary and secondary sources: A Mini-Review.

Resour. Conserv. Recycl. 174, 105813 https://doi.org/10.1016/j.resconrec.2021.105813.
Patakfalvi, R., Diaz, D., Velasco-Arias, D., Rodriguez-Gattorno, G., Santiago-Jacinto, P., 2008. Synthesis and direct interactions of silver colloidal nanoparticles with pollutant gases. Colloid Polym. Sci. 286, 67–77. https://doi.org/10.1007/s00396-007-1702-0.
Pathak, A., Vinoba, M., Kothari, R., 2020. Emerging role of organic acids in leaching of valuable metals from refinery-spent hydro processing catalysts, and potential technoeconomic challenges: A Review. Crit. Rev. Environ. Sci. Technol. 51, 1–43. https://doi.org/10.1080/10643389.2019.1709399.
Pereira-da-Mota, A.F., Vivero-Lopez, M., Topete, A., Serro, A.P., Concheiro, A., Alvarez-Lorenzo, C., 2021. Atorvastatin-eluting contact lenses: effects of molecular imprinting and sterilization on drug loading and release. Pharmaceutics 13, 606. https://doi.org/10.1016/j.cej.2021.130577.
Peris-Martinez, C., García-Domene, M.C., Penadés, M., Luque, M.J., Fernández-López, E., Artigas, J.M., 2021. Spectral transmission of the human corneal layers. J. Clin. Med. 10, 4490. https://doi.org/10.3390/jcm10194490.
Piktel, E., Suprewicz, L., Depciuch, J., Chmielewska, S., Sklodowski, K., Daniluk, T., Krol, G., Kolat-Brodecka, P., Bijak, P., Pajor-Swierzy, A., Fiedoruk, K., Parlinska-Wojtan, M., Bucki, R., 2021. Varied-shaped gold nanoparticles with nanogram killing efficiency as potential antimicrobial surface coatings for the medical devices. Sci. Rep. 11, 12546. https://doi.org/10.1038/s41598-021-91847-3.
Porel, S., Singh, S., Radhakrishnan, T.P., 2005. Polygonal gold nanoplates in a polymer matrix. Chem. Commun. 2005, 2387–2389. https://doi.org/10.1039/B500536A.
Public Health England Ubiquitous Lasers. PHE publications gateway number 2014792 February 2016 https://assets.publishing.service.gov.uk/government/uploads/system/uploads/attachment_data/file/496266/Ubiquitous_Lasers_StdQ.pdf.
Racles, C., Airinei, A., Stoica, I., Ioanid, A., 2010. Silver nanoparticles obtained with a glucose modified siloxane surfactant. J. Nanopart. Res. 12, 2163–2177. https://doi.org/10.1007/s11051-009-9780-1.
Rex, J., Knowles, T., Zhao, X., Lemp, J., Maissa, C., Perry, S.S., 2018. Elemental composition at silicone hydrogel contact lens surfaces. Eye Contact Lens 44, S221–S226. https://doi.org/10.1097/ICL.0000000000000454.
Sakai, T., Alexandridis, P., 2005. Mechanism of gold metal ion reduction, nanoparticle growth and size control in aqueous amphiphilic block copolymer solutions at ambient conditions. J. Phys. Chem. B 109, 7766–7777. https://doi.org/10.1021/jp046221z.
Salih, A.E., Elsherif, M., Alam, F., Yetisen, A.K., Butt, H., 2021. Gold nanocomposite contact lenses for color blindness management. ACS NANO 15, 4870–4880. https://doi.org/10.1021/acsnano.0c09657.
Schneider, C.A., Rasband, W.S., Eliceiri, K.W., 2012. NIH Image to ImageJ: 25 years of image analysis. Nat. Methods 9 (7), 671–675. https://doi.org/10.1038/nmeth.2089.
Sheardown, H., Liu, L., Jones, L., 2006. Chemical characterization of 1–DAY ACUVUE® MOIST(™) and 1–DAY ACUVUE® contact lenses. Invest. Ophthalmol. Vis. Sci. 47, 238. https://iovs.arvojournals.org/article.aspx?articleid=2392236.
Sobianowska-Turek, A., Szczepaniak, W., Zabłocka-Malicka, M., 2014. Electrochemical evaluation of manganese reducers - recovery of Mn from Zn-Mn and Zn- C battery waste. J. Power Sources 270, 668–674. https://doi.org/10.1016/j.jpowsour.2014.07.136.
Sonntag, T., Froemel, F., Stamer, W.D., Ohlmann, A., Fuchshofer, R., Breunig, M., 2021. Distribution of gold nanoparticles in the anterior chamber of the eye after intracameral injection for glaucoma therapy. Pharmaceutics 13, 901. https://doi.org/10.3390/pharmaceutics13060901.
Wang, W., Ren, G., Cai, W., 2015. 3D-Gold superstructures grown on poly(acrylic acid) brush. RSC Adv. 5, 60857–60860. https://doi.org/10.1039/C5RA06547J.
Wang, Y., Wang, T.Y., Wu, L.J., Min, X.B., Liu, H., Wen, D.Q., Ke, Y., Wang, Z.B., Tang, Y. W., Fu, H.K., 2019. Recovery of valuable metals from spent ternary Li ion batteries: dissolution with amidosulfonic acid and D-glucose. Hydrometallurgy 190, 105162. https://doi.org/10.1016/j.hydromet.2019.105162.
Xan, C., Wang, C., Zhu, J., Li, H., 2010. Formation of gold and silver nanostructures within polyvinylpyrrolidone (PVP) gel. J. Solid. State Chem. 183, 858–865. https://doi.org/10.1016/j.jssc.2010.01.021.
Xu, C., Wang, Y., Chen, H., Nie, D., Liu, Y., 2014. Hydrothermal synthesis of silver crystals via a sodium chloride assisted route. Mater. Lett. 136, 175–178. https://doi.org/10.1016/j.matlet.2014.08.038.
Zhang, A.Q., Cai, L.J., Sui, L., Qian, D.J., Chen, M., 2013. Reducing properties of polymers in the synthesis of noble metal nanoparticles. Polym. Reviews 53, 240–276. https://doi.org/10.1080/15583724.2013.776587.
Zhang, D., Ma, J.J., Meng, X.W., Xu, Z.F., Zhang, J., Fang, Y.X., Guo, Y., 2019. Electrochemical aptamer-based microsensor for real-time monitoring of adenosine in vivo. Anal. Chim. Acta 1076, 55–63. https://doi.org/10.1016/j.aca.2019.05.035.
Zhang, Y.W., Peng, H.S., Huang, W., Zhou, Y.Z., Zhang, X.H., Yan, D.Y., 2008a. Hyperbranched poly(amidoamine) as the stabilizer and reductant to prepare colloid silver nanoparticles in situ and their antibacterial activity. J. Phys. Chem. C 112, 2330–2336. https://doi.org/10.1021/jp050136p.
Zhang, Q., Xu, J.J., Liu, Y., Chen, H.Y., 2008b. In-situ synthesis of poly(dimethylsiloxane)–gold nanoparticles composite films and its application in microfluidic systems. Lab Chip 8, 352–357. https://doi.org/10.1039/B716295M.